GEOPHYSICS, VOL. 67, NO. 1 (JANUARY-FEBRUARY 2002); P. 50–59, 11 FIGS., 1 TABLE.
10.1190/1.1451326

Application of a high-resolution seismic investigation in a Greek coal mine

G-Akis Tselentis* and Paraskevas Paraskevopoulos‡

ABSTRACT

High-resolution seismic methods were applied to map the detailed structure and thickness of the Domeniko coal basin (central Greece) and to search for lateral discontinuities, such as pinch-outs and faults. Extensive tests were performed to optimize recording parameters and equipment. Reflection events which can be attributed to coal layers can be interpreted from depths of approximately 30 to 150 m on CDP stacked and inverted sections. Several low-throw faults have been interpreted from the sections. Results obtained from the high-resolution seismic reflection survey combined with drillhole information clearly revealed the 3-D model of the coal field.

Using geostatistical methods, the results of the high-resolution reflection seismic survey were combined with the information from the borehole program to clearly reveal the 3-D model of the basin.

INTRODUCTION

The efficient mining of coal using mechanized methods depends upon an adequate knowledge of the geological structures encountered ahead of the operating face. Even small offsets in the coal seams, on the order of a few meters, caused by tectonic faults can diminish productivity since they severely disrupt the operation of mechanical long-wall mining equipment. Thus, it is imperative that coal companies gather subsurface information.

Seismic exploration has developed alongside the oil industry since the early 1900s. Most of the literature covering seismic exploration techniques is concerned with exploring the depths and structures relevant to oil production.

During the last two decades, high-resolution reflection surveying has been used successfully to evaluate detailed structural and stratigraphic features of coal prospects by a number of investigators employing either 2-D techniques (for example, Ziolkowski and Lerwill, 1979; Ruskey, 1981; Hughes and Kennett, 1983; Greaves, 1984; Harman, 1984; Lawton, 1985; Greenhalgh et al., 1986; Palmer, 1987; Lyatsky and Lawton, 1988; Gochioco and Cotten, 1989; Henson and Sexton, 1991; Gochioco, 1991a,b; Miller et al., 1992; Pîetsch and Slusarczyk, 1992; Gang and Goulty, 1997) or, more rarely, 3-D methodologies (Krey, 1978; Bading, 1986; Lambourne et al., 1990; Urosevic et al., 1992; Walton et al., 1999; Gochioco, 2000).

When combined with drillhole data, high-resolution reflection surveying is a cost-effective method of mapping coal seams for exploration and exploitation. The comparatively continuous subsurface sampling possible with the CDP seismic reflection method has the potential to allow identification of subsurface anomalies significantly smaller than mineral exploration or evaluation drillhole intervals (Miller et al., 1992).

The following case study shows the effective use of seismic data in evaluating the Domenico coal basin (Figure 1). The objectives of the seismic survey were (1) to map the structure of the coal, (2) to map the seam thickness, (3) to locate any faults affecting the coal seam, and (4) to map and interpret any internal discontinuities. It is generally impossible to do this with drillhole data alone, particularly when holes are hundreds of meters apart.

The high-resolution seismic reflection technique cannot replace drilling. However, used in conjunction with a well-planned drilling program, it can significantly increase the knowledge of subsurface geology in less time and at a decreased cost.

GEOLOGIC SETTING

The study area is a small subbasin toward the northern part of the Larissa plain in eastern Thessaly. This region belongs to the Internal Hellenides, which are part of the Greek orogenic belt. The buildup of the entire mountain chain is the result of several compressional events. The last of these events was the Alpide tectonic phase, which affected Thessaly from Eocene to Middle Miocene times.

Manuscript received by the Editor October 26, 1998; revised manuscript received April 30, 2001.
*University of Patras, Seismological Laboratory, Rio 261 10, Greece. E-mail: tselenti@upatras.gr.
‡Formerly University of Patras, Seismological Laboratory, Rio 261 10, Greece; presently LandTech Enterprises, 247 Gray's Inn, London WC1 X8QZ, U.K. E-mail: landtech@landtech.org.

After the Alpide orogeny, the region underwent extensional tectonic conditions, probably related to the postorogenic collapse (Caputo et al., 1994). The area was affected by a northeast–southwest extensional regime. This formed a system of northwest–southeast elongated horsts, grabens, and basins bounded by large normal faults.

The geologic formations encountered in the Domeniko basin are depicted in Figure 1 and can be divided into Neogene formations and Paleozoic formations, the latter forming the boundaries of the basin.

Within the Neogene formations and in depths ranging from 30 down to 150 m, the coal seams are in the form of lignite. Preliminary drilling data showed that the seam thickness ranged from a few centimeters to 20 m. The thickness of the coal seams increases toward the eastern part of the basin, while toward the western part we observe an increase in the number of coal seams with a simultaneous thinning. The seams are not always homogeneous. They are interbedded with sands and clays, especially in the lower part of the lignite zone.

Below the lignite zone we encounter a rather homogeneous sand layer with thickness varying from a few meters to a few tenths of meters lying above a formation of conglomerates on top of the metamorphic basement.

DATA ACQUISITION

With the exception of scale, the CDP seismic reflection methodology used here was similar to the method as applied to petroleum exploration.

The quality of high-resolution shallow reflection surveys is strongly dependent on the field parameters (e.g., Knapp and Steeples, 1986) and the selection of an appropriate energy source (Miller et al., 1994). Data for this investigation were acqired on a 120-channel Jupiter 24-bit seismograph from Bison,

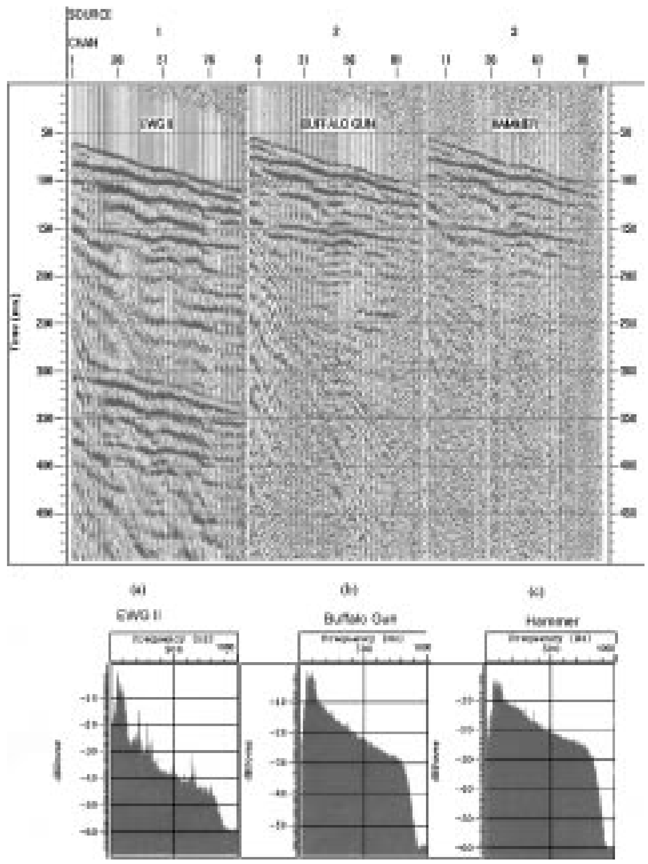

FIG. 2. Seismic data generated by (a) EWG-II accelerating weight drop, (b) buffalo gun, and (c) sledgehammer. Corresponding amplitude spectra are also shown.

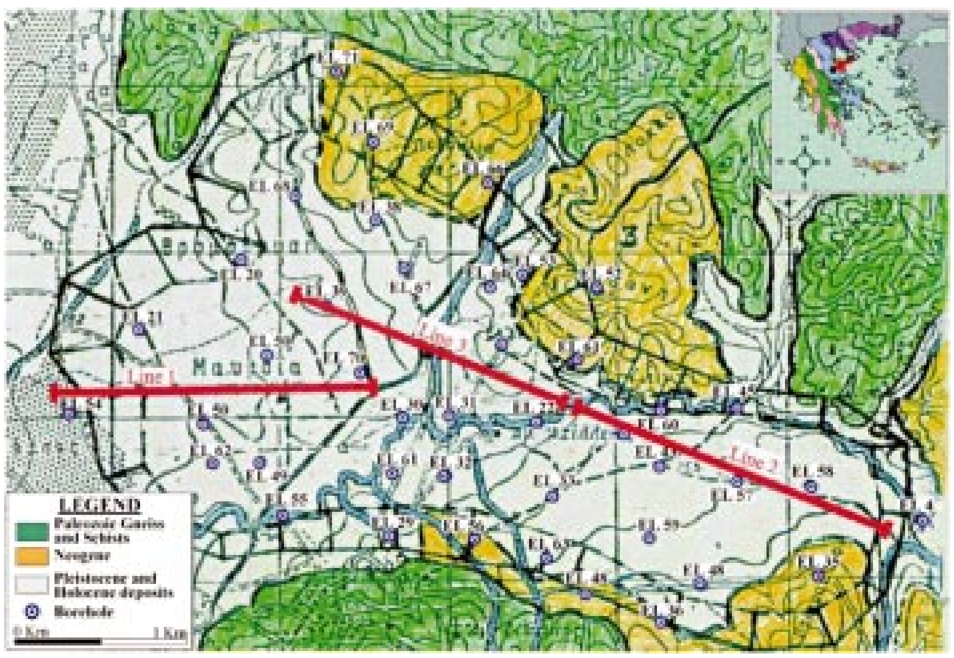

FIG. 1. Geological map of Domeniko coal basin, showing the location of the seismic lines and boreholes.

using single 60-Hz geophones spaced at 5-m intervals. The seismograph amplified, filtered, and then digitized the analog signal into a 24-bit word and stored the digital information in a demultiplexed format. Proper matching of high- and low-cut filters for the acoustic characteristics and targets optimized the seismograph's dynamic range.

A minimum of four octaves in frequency was considered enough for the desired resolution. Therefore, the production line was acquired with 50-Hz analog low-cut and 825-Hz analog high-cut two-pole Butterworth filters. The 825-Hz high-cut filter was also the system antialias filter for the 0.5-ms sample period ($f_N = 1$ KHz).

Synthetic seismograms calculated using nearby drillhole data provided preliminary estimates of the two-way reflection times for the coal seams and were used to help design field parameters prior to the actual start of the survey.

The recording of field data was preceded by extensive tests involving walkaway and source investigations. Both an 8-inch gauge buffalo gun (Pullan and MacAulay, 1987) and a Bison EWG II accelerating weight drop were used as seismic sources.

When the buffalo gun was used (in cases where the terrain prohibited the use of the EWG II), small-diameter holes were drilled to a depth of 1.5 m and were filled with water to damp the air blast and confine energy in the ground during detonations.

When the accelerating weight drop was used, ten strikes on average were stacked at each shotpoint to enhance the S/N ratio. Typical raw field files from these seismic sources are depicted in Figure 2 and compared with sledgehammer data. Reflections, refractions, ground roll, air-coupled waves, and mode-converted energy can be identified on the raw field data. The best results were obtained using the EWG-II as a seismic source. The other two sources did not have the required energy to produce reflections that were clear enough at later times.

Unequivocal identification of reflection energy on field data is essential for accurate interpretation of CDP stacked sections. Reflections can be interpreted on short-offset data as shallow

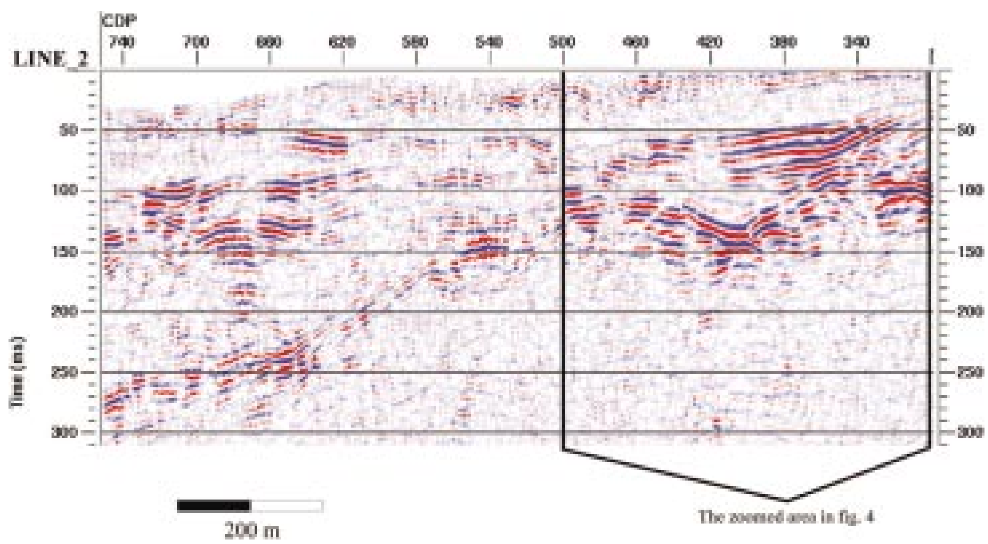

FIG. 3. Seismic section of part of seismic line 2 plotted using variable density.

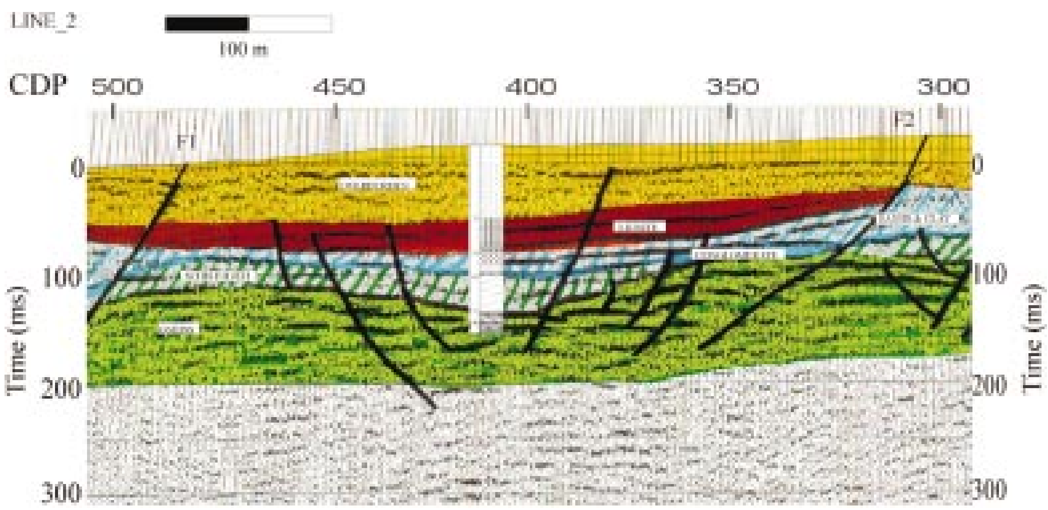

FIG. 4. Expanded interpreted portion of the section marked in Figure 3. The borehole data were converted in time; but the values appearing in the geologic column include the corresponding depth in meter.

as 70 ms and as deep as 400 ms (Figure 2). The determination of source, receivers, source–receiver offset, and analog filter settings was based on a combination of qualitative and quantitative analyses of the data.

All previous tests showed that high-quality data could be obtained using the acquisition parameters summarized in Table 1.

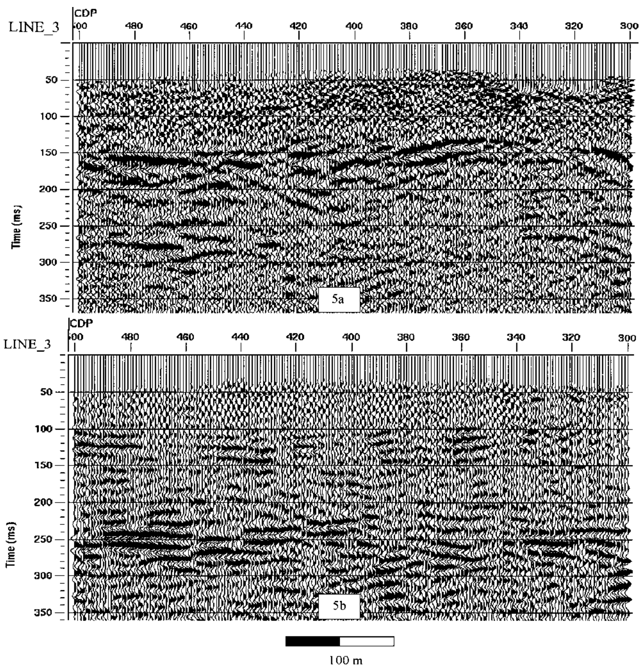

FIG. 5. Part of the processed section of line 3 with (a) elevation statics only and (b) refraction statics and time-variant filtering.

DATA PROCESSING

The resolution required for coal-seam mapping is on the order of a few meters, both vertically and laterally. The field, processing, and interpretation procedures differ significantly from those in seismic exploration for oil and gas. The survey must be accurately and judiciously specified to determine the cost benefit of seismic reflection profiling relative to increased density of drilling, notwithstanding the continuity of subsurface sampling and other advantages offered by seismic mapping.

The data were processed on a Sun workstation using Promax-3D and Hampson-Russell Software's GLI-3D and Strata-3D processing packages. The processing flow was similar to that used in petroleum exploration. Data characteristics and scale, unique to shallow reflection data, required a conservative approach to correlation statics, velocity and spectral analysis, and

Table 1. Data acquisition parameters.

Parameter	Value
Seismic source	Bison EWG-II accelerating weight drop (main part), buffalo gun
Recording system	Bison Jupiter seismograph
Sample rate	0.5 ms
Record length	750 ms
Number of channels	96
Receiver	Single, 60-Hz geophone
Spread type	Split spread
Maximum fold	48
Geophone interval	5 m
Source interval	5 m
Low-cut analog filter	50 Hz
High-cut analog filter	825 Hz
Recording format	SEG2

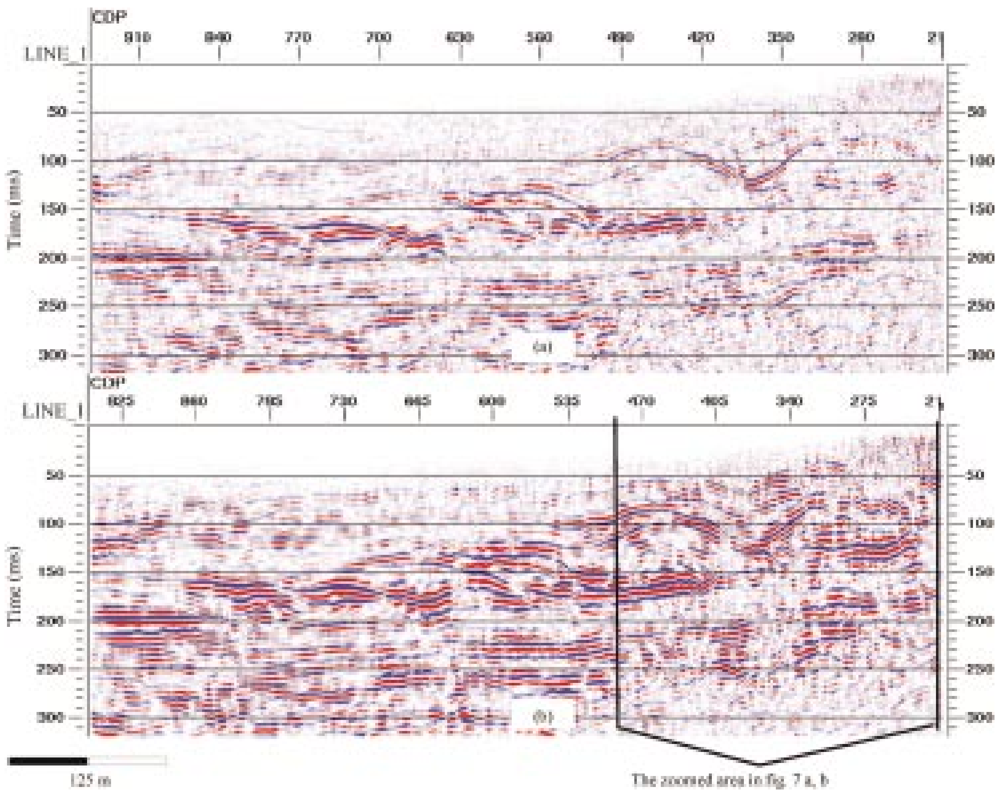

FIG. 6. (a) Unmigrated and (b) migrated portions of line l.

trace-by-trace muting and deconvolution. The field static applications, crucial to shallow seismic reflection interpretation (Ziolkowski and Lerwill, 1979), were determined by separate refraction spreads shot along each profile.

The main processing steps were as follows:

1) assignment of field geometry, surface-wave noise attenuation (assuming an apparent velocity of 360 m/s and a 0–50-Hz bandwidth), air-blast attenuation (assuming a wave velocity of 331 m/s), trace editing, and muting;
2) amplitude adjustments by spherical divergence corrections, f–k filtering, minimum-phase spiking deconvolution (with an operator of 100 ms and 1% white noise), band-pass filtering (50–150 Hz), and application of static corrections;
3) velocity analysis, NMO corrections, top mute, and common midpoint stacking;
4) deconvolution after stack, time-variant filtering, and migration (finite difference in time); and
5) inversion of the data.

COAL-SEAM REFLECTIVITY AND RESOLUTION

To determine the most appropriate techniques with which to conduct a high-resolution shallow seismic reflection survey over a coal field and the criteria for geological interpretation of the seismic data, synthetic seismograms were compiled, taking into consideration representative material properties. The density values of the geological formations were assessed from measurements on core samples. Seismic velocities were assessed both from core and in-situ measurements.

Average values of density (ρ) and layer velocity (V) computed for the Domeniko basin were $\rho \sim 13$ g/cm^3, $V \sim 1800$ m/s for coal and $\rho \sim 1.9$ g/cm^3, $V \sim 2000$ m/s for host sedimentary

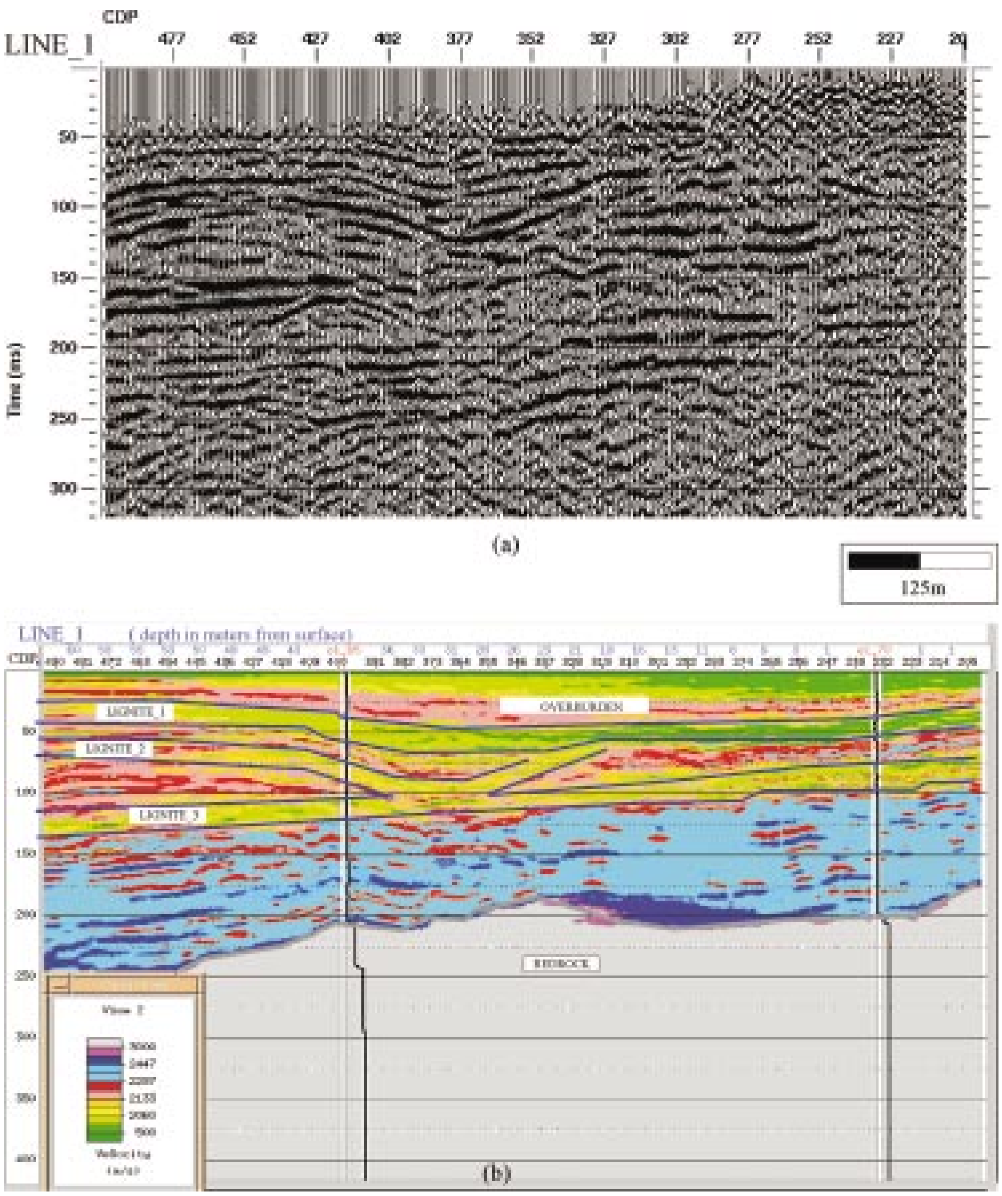

FIG. 7. (a) Observed data between CDP 202–500 for line 1; (b) 2-D inverted model. Vertical scale is in meters.

rocks. Reflection coefficients are typically about ±0.25, so coal seams can be considered good reflectors.

An important factor in a multiseam environment is that not only do the large reflection coefficients cause high-amplitude primary reflections but that strong surface multiples and interbed multiples are also set up within and between seams (Greenhalgh et al., 1986). This broadens the seismic pulse as a result of tuning effects, lowers frequency content because of absorption, and generates a train of short-period multiples.

It is important to point out the difference between resolution and detection in seismic data analysis (Greaves, 1984). Resolution is limited by the minimum thickness of a layer in which the top and bottom produce clearly observable effects and is defined as one-quarter of the wavelength of the dominant frequency in the reflector of interest. On the other hand, the detection limit is defined as the minimum thickness for the seismic response from a layer to be distinguished and is estimated as one-thirtieth of the wavelength. Of course, the practical limits for a particular data set depend on S/N ratio and the judgment of the seismic interpreter.

The typical dominant frequency of the reflector from the Domeniko coal field was estimated at around 90 Hz. An estimated interval velocity of 1900 m was used to determine the resolvable limits, yielding a value of 4 m and a detection limit on the order of 1m for a thin bed.

As far as faults are concerned, the detection limit is better than the resolvable limit. If a vertical displacement of the seismic trace on the order of 3 ms can be detected, a fault with 3 to 4 m of displacement will be identified.

RESULTS

Reflections from the coal seams were detected along almost all of the seismic lines. Figure 3 shows the final processed section (plotted in variable density) between CDPs 300 and 750 of line 2. Coherent reflections can be interpreted across almost the entire line. The weakening of the amplitude of the reflected waves observed between CDPs 500 and 620 is because the EWGII was replaced by a buffalo gun at this part of the line because of accessibility problems. The CPD stacked section has a maximum nominal fold of 48. The metamorphic bedrock is clearly depicted with a westward dip.

Figure 4 is an expansion of a portion of Figure 3, which represents the eastern part of line 2. The interpretation of the section depicted in Figure 4 is based on a borehole drilled at CDP 414, which encountered the lignite zone between 58 and 84 m. Next follows a layer of sands and clays up to 106 m. Then a 24-m-thick conglomerate layer is encountered on top of the metamorphic (gneiss) basement at a depth of 130 m. The continuity of the events is interrupted in many locations along the entire section. These discontinuities were interpreted as shallow faults with minor vertical displacements. Faults Fl and F2 can be traced to the surface and have been recognized during geological reconnaissance.

The coal reflection is interpreted to be present at approximately 65 ms. Reflections interpreted to represent acoustic interfaces at or near the coal depth are almost horizontal along the entire line up to CDP 500.

It is important to remove the effects of the surface low-velocity layers, encountered all over the investigated region. To derive the near-surface effects we used GLI-3D generalized linear inversion refraction routines. This iterative, model-based approach provides flexibility in defining a near-surface model consisting of arbitrarily parameterized multilayers. The process begins by computing the refracted arrival times from an assumed initial near-surface model. These computed traveltimes are then compared with the actual first-break picks and the difference is minimized by modifying iteratively the

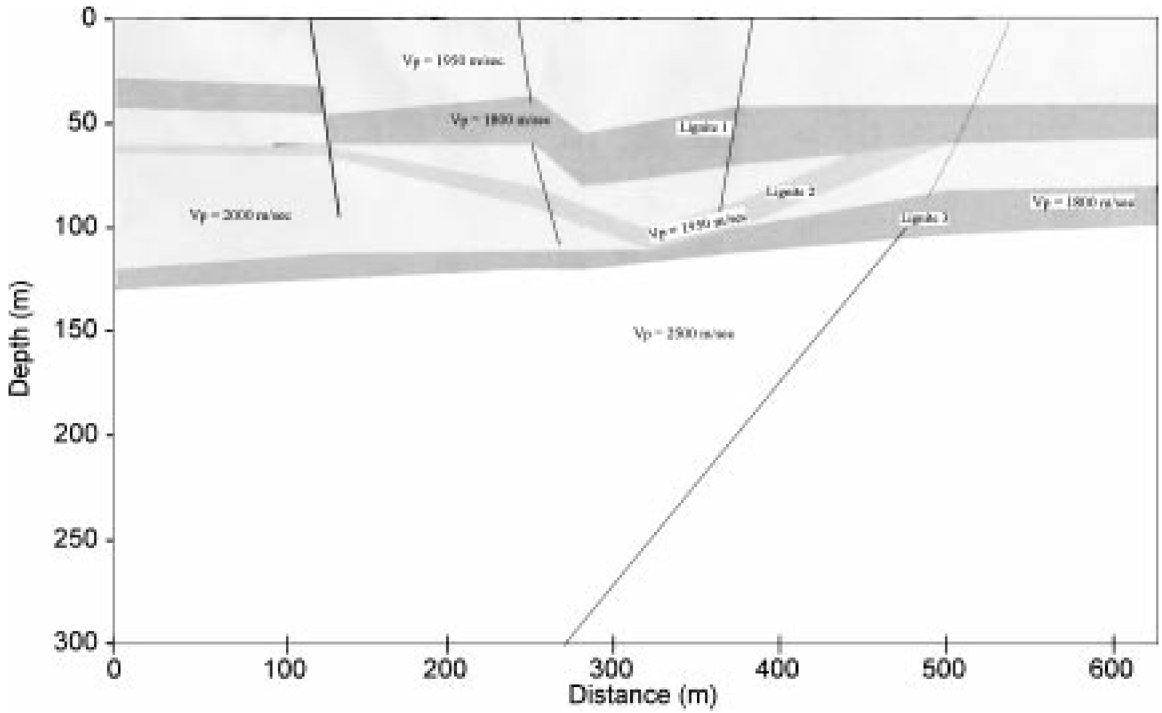

FIG. 8. Simplified structural/geologic model used to create synthetic traces with the finite-differences method. The metamorphic basement is not included in this model.

near-surface model parameters. Figure 5a shows part of seismic line 3 between CDPs 300 and 500 with elevation statics only. The application of generalized linear inversion refraction statics in combination with time-variant filtering results in a more coherent appearance of the target coal seams (Figure 5b).

Figure 6a shows the final processed (unmigrated) portion of line 1 between CDPs 210 and 966. Figure 6b shows the same data after finite-difference time migration. The coherence of the reflectors has being increased, and various diffraction features encountered in Figure 6a (e.g., at CDP 420, 170 ms) have been collapsed. Figure 7a is an expansion of a portion of Figure 6b, displaying the migrated data between CDPs 202 and 500. Stratigraphic and lithologic information is obtained from boreholes el 70 and el 65 drilled close to CDPs 232 and 400, respectively.

Next we attempted to apply the poststack generalized linear inversion (GLI) method to the migrated section depicted in Figure 7a to reconstruct the velocity structure of the entire section and obtain a better picture of the distribution of the coal field. We used the blocky inversion algorithm of Strata-3D software. To our knowledge the only other attempt to apply the GLI method to thin-bed exploration is by Gang and Goulty (1997).

We consider that, as far as possible, our processing sequence preserved true relative amplitude and a uniform bandwidth down the section. Velocity and density measurements in both boreholes were used to construct acoustic impedance logs with reference to the corresponding lithological log. Synthetic traces, generated using the extracted wavelet and the reflection coefficient sequence from the acoustic impedance log, were compared with observed traces through a crosscorrelation process. The derived 2-D velocity inverted section of line 1 between CDPs 202 and 500 is depicted in Figure 7b.

The inversion results combined with the borehole data were next used to construct a 2-D block model suitable for finite-difference numerical modeling. This model (Figure 8) features three coal seams. The numbered layers mark, from the top, the surface low-velocity layer ($V_p = 800$ m/s) and three coal seams ($V_p = 1750, 1950,$ and 1850 m/s). The upper coal seam is faulted at the left side of the section (blocks 3 and 11). A velocity ratio $V_p/V_s = 4.3$ is assumed throughout the model.

Figure 9a presents the obtained finite-difference section of the model depicted in Figure 8, in which the complete elastodynamic equation was solved using a Gabor wavelet of 100 Hz as a source signature (e.g., Zahradnik and Bucha, 1998).

Figure 9b shows the results of the migration algorithm on the synthetic data. As in the case of the real field data, finite-difference time migration was used. From the two synthetic sections in Figure 9, three results become clear. The P-reflections dominate the section, both the reflections from the top and bottom of the coal seams are seen, and the converted waves and multiples complicate the picture. The bedrock was not considered in this finite-difference model, i.e., the lower coal seam is underlain by a homogeneous medium encountering a P-velocity of 2800 m/s. In other words, we restricted our modeling to the time before the bedrock reflection arrived.

Comparing the synthetic sections (Figure 9) to the true section (Figure 7a) we conclude that the main features of the structural model have been validated, at least in a qualitative sense. This includes not only the main top (first) and bottom (third) coal seam but also the intermediate seam. At least in the left part of the profile, this intermediate coal seam seems to be separated from the upper coal seam.

The interpreted final stacks of all three lines are depicted in Figure 10. Figures 10a–c are the interpretations for lines 1–3, respectively. Coherent reflections can be interpreted across the stacked sections. The coal seams are not uniform and are disrupted by various pinch-outs and faults. The drilled boreholes confirm the accuracy of the seismic results, and subtle stratigraphic features can be interpreted on many parts of the sections. Variations in amplitude and frequency of the coal reflection could indicate changes in bed thickness or lithologies. Such an example is the western part of line 2 between CDPs 900 and 1000 where the coal field takes the form of many thin coal seams interbedded with sands and clays.

Various normal faults have been interpreted down to the metamorphic basement. These structures account for about 3 to 6 m (about 2 to 4 ms two-way time) of vertical change in

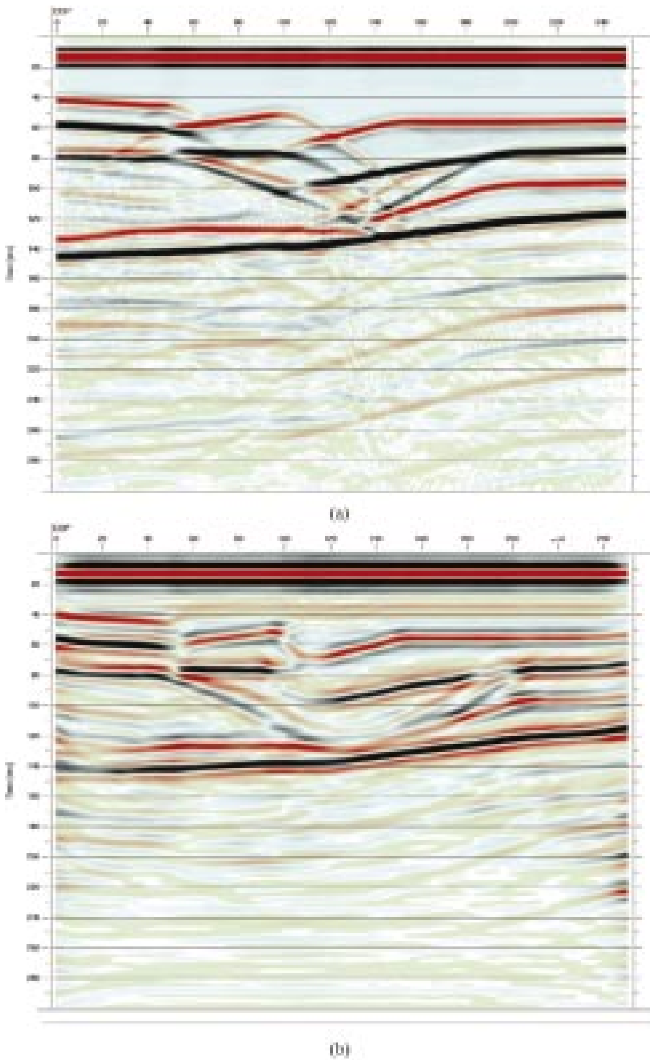

FIG. 9. (a) Synthetic traces generated from the model depicted in Figure 8. The section was created assuming 1251 sources at the surface 0.5 m apart, all acting simultaneously. The complete 2-D wavefield is considered, including all multiples and conversions existing in the model. (b) Section (a) with finite-difference time migration applied.

the coal elevation. The basement is also clearly depicted apart from a small section between CDPs 800 and 950 in line 2.

This effect on the reflector of the bedrock can be attributed to the presence of a major fault that appears at the surface as the riverbed that separates lines 2 and 3 (Figure 1). This fault also causes the discontinuity between the western part of line 2 and the eastern part of line 3.

The final stage of the interpretation was the use of geostatistical methods to combine the results of the seismic survey and the drilling program to construct a 3-D representation of the Domeniko coal field. Considerable effort was put toward selecting the most adequate kriging methodology.

Kriging is a weighted moving average interpolation (extrapolation) method which minimizes the estimated variance of a predicted point (node) with the weighted average of its neighbors (e.g., Clark 1994). The weighting factors and the variance are calculated using a variogram model which describes the differences versus distance for pairs of samples in the input data set. The latter consists of a series of geological pixels (obtained from borehole data or from the seismic model) describing the geological layers in x-y-z Cartesian space. We used adaptive gridding, which automatically refines gridding in the cells surrounding measured samples to ensure that the interpolated results and isosurfaces accurately honor measured sample data.

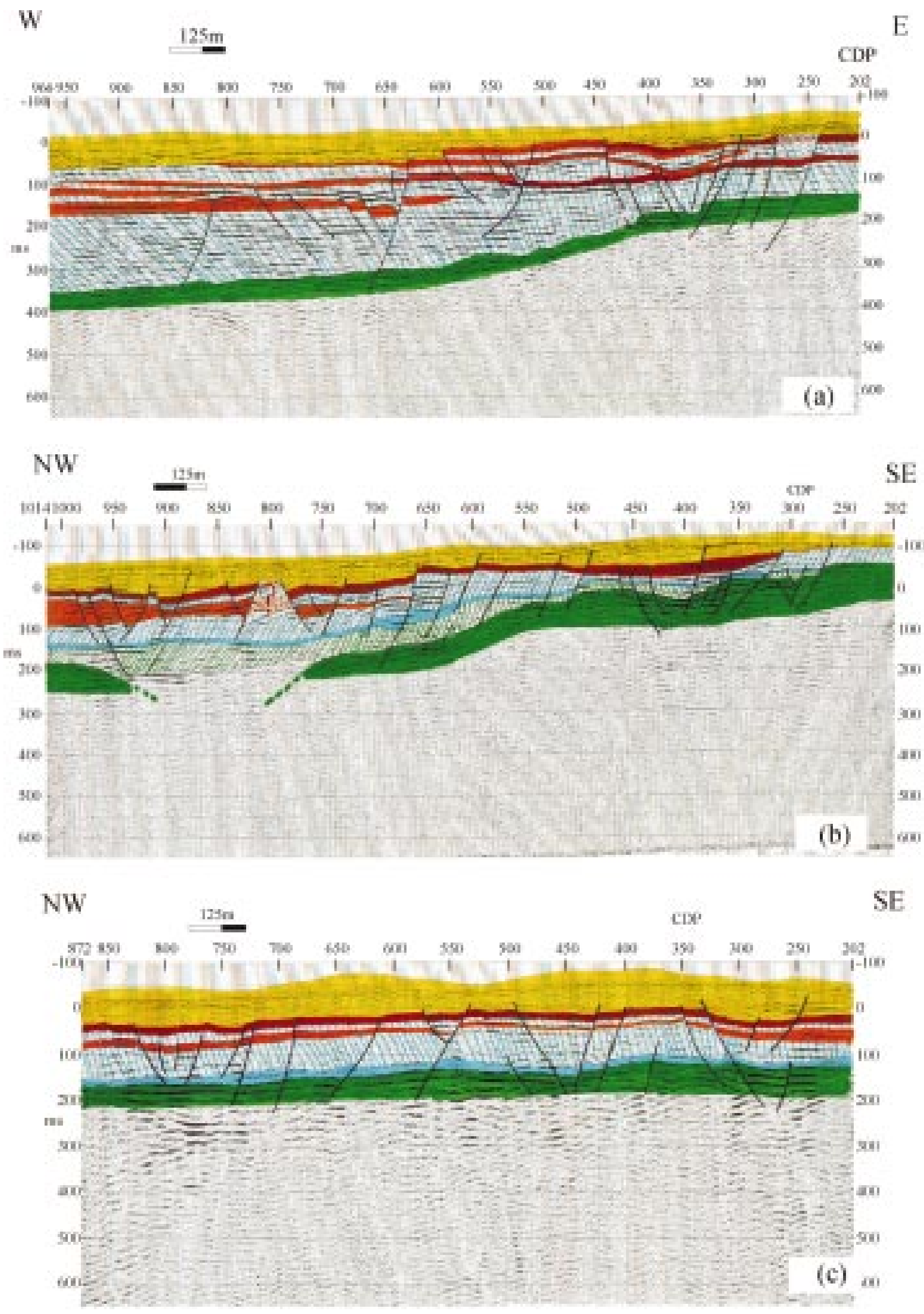

FIG. 10. Interpreted sections of (a) line 1, (b) line 2, and (c) line 3.

The process of determining an appropriate variogram is one of the most serious parts of the modeling process. Instead of following the traditional approach, which considers the differences between samples versus their distance from one another, we followed a new approach—extending this concept by also considering the direction (vector distance). This methodology is capable of better representing coal seam trends in the data.

The complete 3-D model of the Domeniko coal field is presented in Figure 11a. Similar views after removing the overburden above the first coal seam and the material above the second coal seam are depicted in Figures 11b and 11c, respectively.

CONCLUSIONS

Drilling practices common to the coal industry cannot provide the required geological information for effective coal-mine planning. When surface seismic surveys are used in conjunction with drilling, subsurface geological information can help mine engineers develop optimal mine plans.

The results of the high-resolution seismic reflection survey carried out in the Domeniko coal basin enabled the detection and mapping of the lateral extension of the coal seams effectively. All the main geological interfaces were mapped accurately, and several low-throw faults were interpreted from the seismic sections. The results have been verified both by inverse modeling and drilling.

ACKNOWLEDGMENTS

The authors thank Helmut Gaertner, Neil Goulty, and Reimund Seitz for their time, discussions, and suggestions during our research. Special thanks are extended to Jiri Zahradnik, who wrote the finite-difference code used in the numerical simulation. Asbjorn N. Christensen, Shanti Rajagopalan, and two anonymous reviewers are also aknowledged for their constructive comments. The Greek Public Power Corporation supported the coal geophysics program and granted permisson to release this paper for publication. LandTech Enterprises supplied vital equipment during the field work. The contribution of Andreas Sotiriou, George Manos, and Yanis Zepos is also acknowledged. The project was financed by the NATOsfs/GRCOAL and CEC/SHIELDS/NNE5/1999/381 projects.

REFERENCES

Bading, R., 1986, How to optimize 3-D seismic land surveys—Some rules for areal data gathering, *in* Buchanan, D. J., and Jackson, L. J., Eds., Coal geophysics: Soc. Expl. Geophys. Reprint **6**, 211–236.

Caputo, R., Bravard, J., and Bruno, H., 1994, The Pliocene-Quaternary tecto-sedimentary evolution of the Larissa plain (eastern Thessaly, Greece): Geodinamica Acta (Paris), **7**, No. 4, 219–231.

Clark, L., 1994, Practical Geostatistics: Applied Science Publishers, London, 435.

Gang, T., and Goulty, N. R., 1997, Seismic inversion for coal seam thicknesses: Trials from the Belvoir coalfield, England: Geophys. Prosp., **45**, 535–549.

Gochioco, L. M., 1991a, Advances in seismic reflection profiling in U.S. coal exploration: The Leading Edge, **10**, No. 12, 24–29.

——— 1991b, Application of the seismic interactive interpretation workstation for the coal industry: Mining Eng., **43**, 1057–1061.

Gochioco, L., 2000, High-resolution 3-D seismic survey over a coal mine reserve area in the U.S.—A case study: Geophysics, **65**, 712–718.

Gochioco, L., and Cotten, S., 1989, Locating faults in underground coal mines using high-resolution seismic reflection techniques: Geophysics, **54**, 1521–1527.

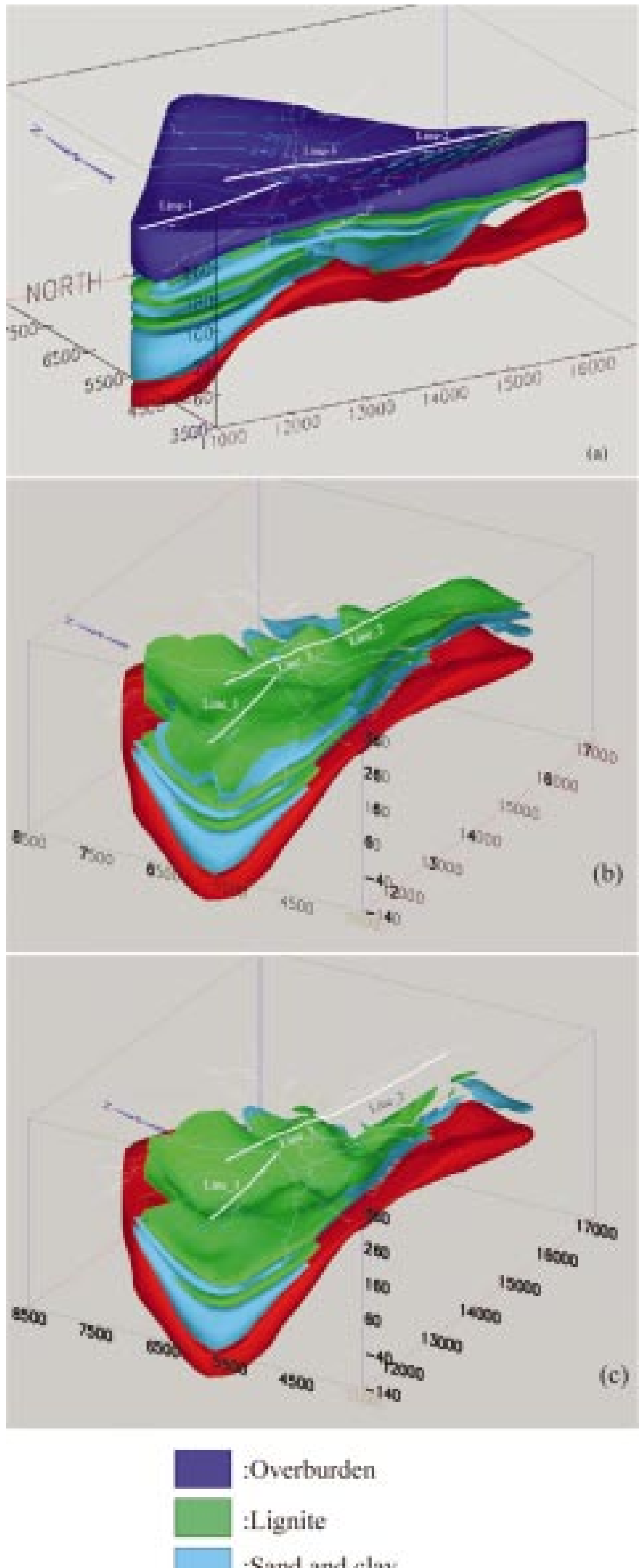

FIG. 11. (a) A 3-D model of the Domeniko coal basin. (b) The same model without the overburden. (c) The same model without the formations above the second coal seam. The distance in the grid is in meters.

Greenhalgh, S., Suprajitno, M., and King, D., 1986, Shallow seismic reflection investigations of coal in the Sydney basin: Geophysics, **51**, 1426–1437.

Greaves, R. J., 1984, Coal-prospect evaluation using high-resolution reflection seismology, a case study: The Leading Edge, **3**, 44–47.

Harman, P. G., 1984, High resolution seismic reflection techniques applied in coalfields: Cook Colliery, Queensland—A case history: Expl. Geophys., **15**, 220–228.

Henson, H., Jr., and Sexton, J. L., 1991, Premine study of shallow coal seams using high-resolution seismic reflection methods: Geophysics, **56**, 1494–1503.

Hughes, V., and Kennett, B., 1983, The nature of seismic reflections from coal seams: First Break, **2**, 9–18.

Knapp, R. W., and Steeples, D. W., 1986, High-resolution common-depth-point seismic-reflection profiling: Field acquisition parameter design: Geophysics, **51**, 283–294.

Krey, T., 1978, Reconciling the demands of 3-D seismics with those of improved resolution: Presented at 48th Ann. Internat. Mtg., Soc. Expl. Geophys.

Lambourne, A. N., Evans, B. J., and Hatherly, P., 1990, Areal coal seam mapping by 3-D seismic reflection surveying: A case history from the Sydney basin, Australia: 60th Ann. Internat. Mtg., Soc. Expl. Geophys., Expanded Abstracts, 726–728.

Lawton, D., 1985, Seismic facies analysis of delta-plane coals from Camrose Alberta, and lacustrine coals from Pictou coalfield, Nova Scotia: AAPG Bull., **69**, 2120–2129.

Lyatsky, H., and Lawton, D., 1988, Application of the surface seismic reflection method to shallow coal exploration in the plains of Alberta: Can. J. Expl. Geophys., **24**, No. 2, 124–140.

Miller, R. D., Pullan, S. E., Keiswetter, D. A., Steeples, D. W., and Hunter, J. A., 1994, Field comparison of shallow *P*-wave seismic sources near Houston, Texas: Geophysics, **59**, 1713–1728.

Miller, R. D., Saenz, V., and Huggins R. J., 1992, Feasibility of CDP seismic reflection to image structures in a 220-m deep, 3-m thick coal zone near Palau, Coahuila, Mexico: Geophysics, **57**, 1373–13811.

Palmer, D., 1987, High resolution seismic reflection surveys for coal: Geoexpl., **24**, 397–408.

Pîetsch, K., and Slusarczyk, R., 1992, The applications of high-resolution seismics in Polish coal mining: Geophysics, **57**, 171–180.

Pullan, S. E., and MacAulay, H. A., 1987, An in-hole shot gun source for engineering seismic surveys: Geophysics, **52**, 985–996.

Ruskey, F., 1981, High-resolution seismic methods for hard-rock mining: U.S. Bur. Mines Info. Circ. **8891**, 4–28.

Urosevic, M., Evans, B. J., and Hatherly, P. J., 1992, Application of 3-D seismic methods to the detection of subtle faults in coal seams: 62nd Ann. Internat. Mtg., Soc. Expl. Geophys., Expanded Abstracts, 254–256.

Walton, C., Evans, B., and Urosevic, M., 1999, Seismic methods for delineating complex structures in coal seams: 69th Ann. Internat. Mtg., Soc. Expl. Geophys., Expanded Abstracts, 1422–1425.

Zahradnik, J., and Bucha, V., 1998, Masking effects of subsurface layers on shallow reflecting horizons: J. Seismol. Explor., **7**, 73–79.

Ziolkowski, A., and Lerwill, W. E., 1979, A simple approach to high resolution seismic profiling for coal: Geophys. Prosp., **27**, 360–394.